MODULARIZED BIDIRECTIONAL STEP-UP DC-DCD CONVERTER WITH PREDICTIVE BATTERY EQUALIZATION METHOD

Edson J. Lorencetti and Joselito A. Heerdt
Santa Catarina State University – UDESC
Electric Power Processing Group – nPEE
89.219-710, Joinville – SC, Brazil
edsonlorencetti@gmail.com, joselito.heerdt@udesc.br

Abstract – Battery systems that require higher voltage outputs use to face the problem of State of Charge (SOC) equalization of the cells, which causes premature deterioration of the batteries. This paper proposes a modularized system based on a bidirectional boost converter and an intelligent control of charge and discharge of the battery system based on predictive control system. The main objective of this system is to maintain all cells or banks in an equal charge in order to improve their health and total energy capacity available to use. This system can be used as an alternative method to the common series connected batteries systems.

Keywords — Battery Equalization, Energy Balancing, Batteries, Electric Vehicles, Boost bidirectional converter

I. INTRODUCTION

There are many electrical applications that require a high number of battery cells connected in series to achieve the desired voltage of the DC bus of the system, such as Uninterruptable Power Supplies (UPS) and Electrical Vehicles (EV). Despite of the series configuration of the battery bank, the rates of charges and discharges of every cell are not quite equal to each other due to the factors which are essentially related to small differences between internal parameters of batteries and external conditions of operation across each cell.

The unbalancing of the energy through the system results in an unbalanced internal heating of the cells, and this stress can be dangerous for some kind of batteries which have specific thermal limits that must be respected during its operation, as it occurs on lithium batteries technologies. Another relevant drawback of the SOC imbalance is the effects on State of Health (SOH) of the battery [1-3].

In order to prevent the negative impacts on batteries as a result of the SOC unbalancing, dissipative equalization circuits used to be integrated to the battery system to throw out the exceed energy of the most charged cells of the bank. Despite of the low cost of this solution, it has low energy efficiency, and the equalization process can become slow depending on the quantity of series connected cells and the energy gap between the cells with higher and lower charges. But there are also active equalization approaches that results in a more efficient and faster process, such as flying capacitor or DC/DC topologies which have the role to transfer the energy of the most charged cells to the lower ones. These techniques can be divided basically in three types: *Individual*: which transfer energy from one cell to another [4-7]; *Modularized*: which transfer energy from a group of series cells to another group [8-10]; *Hybrid solutions*: which use other system to exchanged energy with the cell, such as intelligent solution using supercapacitors bank– as studied in [11-13].

In this paper is proposed a modularized DC-DC converter system based on a bidirectional boost converter that can be used as an individual or modularized active equalizer. It's based on building block systems that exclude the necessity of a central power converter [14]. The control method used is based on state-space model predictive control (SSMPC) and it monitors the parameters of the batteries and predicts the future values of SOC and internal temperature of the banks of cells. Through this prediction the main controller is able to configure the voltage reference of each converter control in order to balance the SOC and temperature of the bank. The system can be used as a modularized or individual equalizer and operates during the charges and discharges of the system, eliminates use of additional converters operating as equalizers. This results in reducing energy losses.

An individual equalizer using four lead-acid batteries will be used to simplify the study, and simulations will be shown. The topology of the step-up converter is illustrated in Fig. 1.

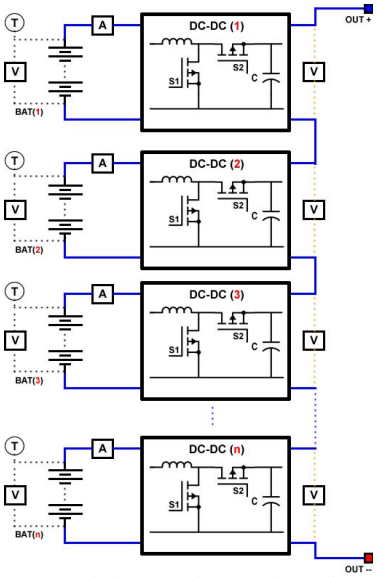

Fig. 1 – The proposed charge, recharge and equalization topology

In case of using more than one cell per converter (system operating as a modularized equalizer), the equalization will occur between batteries bank only. To equalize the individual cells an external equalizer will be necessary.

978-1-5090-6248-5/7/$31.00 © 2017 IEEE

II. PROPOSED CHARGE AND DISCHARGE SYSTEM AND THE EQUALIZER

The proposed system is modularized, where each converter output is connected in series to the output of the next converter. These converters are responsible to step-up its own associated battery voltage and keep the voltage of DC link stabilized and they operate. They also operate as a charge equalizer over the charges and discharges of the batteries.

This process is realized through the constant monitoring of electrical and thermal parameters of the batteries which will provide the entries of the main controller. This higher level controller sets the output reference voltage, $v_{ref}(n)$, for each converter control.

A. Bidirectional DC/DC converter – Discharge mode

The Boost converter with two switches is used in the discharger mode of the system, and the first stage of the operation, $S_1(n) = \overline{S_2(n)} = 1$, is showed in Fig. 2a. The process occurs during the period of time, $0< t \leq DT$, where the magnetic energy of the inductors L(n) are increased linearly with a slope of $V_{in}(n)/L(n)$. As long as it happens the capacitors C(n) transfer energy to the load. In the second stage of operation, $S_1(n) = \overline{S_2(n)} = 0$, that occurs at $DT< t \leq T$ the capacitor C(n) and the load receive energy from the battery and the Inductor L(n), as it is showed in Fig. 2.b.

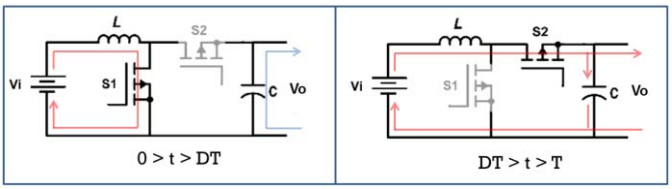

Fig. 2 – Boost Converter: (a) 1º stage (b) – 2º stage

B. Bidirectional DC/DC converter – charger mode

The flux of energy can be reversed allowing the system operates in a regenerative or rechargeable mode, both transferring energy from DC link to the batteries. The system, in these cases, operates as Buck converter, where the switches $S_1(n)$ stay opened during recharging. During the first stage, $0< t \leq DT$, the energy is transferred from DC link to the batteries and during the second stage the flux is cut off as it is possible to see in the Fig. 4a and Fig. 4b.

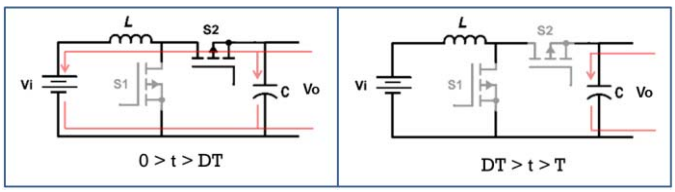

Fig. 3 – Buck Converter: (a) 1º stage (b) 2º stage

C. Process of Equalization through the discharge mode

Considering all converters operating with the same control characteristics, the energy transferred to the load by each one of them will tend to be very similar. However, during the unbalanced SOC situations the less-charged cells will naturally lose its full capacity before the others, and that might cause a great thermal and electrical stresses and result in a premature turn-off of the system. To prevent this, the main controller is design to frequently update the voltage references, $v_{ref}(n)$, of the converters, by making the cells with higher level of SOC provide more energy to the load. At that same time those cells with lower SOC level will provide less energy to the load, and consequently operate for longer time with lower energy and thermal stresses. Fig. 4 shows this operating mode.

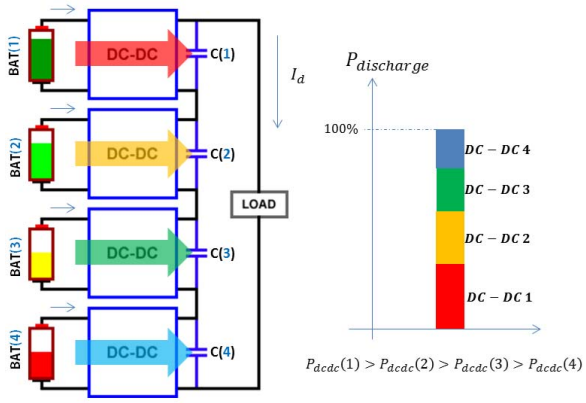

Fig. 4 –Equalization operation during the discharge mode

D. Process of Equalization through the recharge mode

In a similar way of the discharge mode, the reference voltage of each converter is defined by the main controller in order to transfer more energy from the DC link to the batteries with lower level of energy accumulated, as shown in Fig. 5.

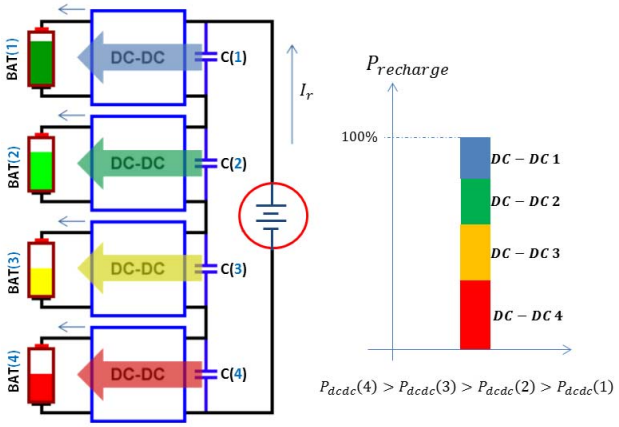

Fig. 5 –Equalization operation during the recharge mode

III. MODELING OF THE PARAMETERS

Only the discharge mode configuration will be validated in this paper.

A. State of Charge (SOC)

The state of charge of batteries can be a difficult task to estimate because the internal parameter change by temperature and load variations. Some methods are proposed in [15]-[18]. The coulomb counting method is the mathematic model used in the predictive calculations to estimate the future state of SOC. The variation of SOC is estimated through the integration of the current in a small period of time, as shown in expression above. [15-16]

$$\Delta SOC = \frac{1}{\beta(T).Cap}\int_{ti}^{tf}\eta(I).I.dt \qquad (1)$$

The factors $\beta(T)$ and $\eta(I)$ represent the system´s dependency on temperature and load respectively. The period of time, $tf - ti$, must be short to reduce the accumulated error, which can be very high in this technique.

B. Internal temperature (Te)

The equalizer function proposed has the objective to keep all SOC as close as possible to optimize the total capacity of the battery bank and also to maintain the lifetime of the batteries. Since some batteries can operate for a long period of time with higher rates of discharge/charge than other batteries, they also can suffer greater thermal stresses which could shorten the lifespan of these batteries. Then, consider the monitoring of the internal temperature variation in the main controller is important to helping set the thermal limit of operation of each cell. The analysis of the temperature can be divided in two parts [15]-[19]. The first part represents the internal variations cause by the joule effects and the second is related to difference between internal and external temperature.

$$\Delta\theta = \Delta\theta_{int} - \Delta\theta_{ext} \qquad (2)$$

The variation of the internal temperature can be expressed by,

$$\Delta\theta = \int_0^t \left[\frac{P_s}{C_o} - \frac{\theta - T_a}{C_o R_o}\right] dt \qquad (3)$$

The power losses of the cells are present by Ps, and Co e Ro which are the electrical and thermal parameters of the batteries.

C. Internal parameters of the batteries

The internal losses of a battery depend on temperature and current flow. The greater is the flux energy from the battery to the load, the greater will be the losses in this battery, and in the practice it can be understood as a reduction of the capacity available. In this study, this dependency is simplified by a linear behavior, $\eta = A_{fc}I + B_{fc}$.

IV. PROPOSED DIGITAL CONTROL METHOD

Fig. 6 shows the general control scheme of the circuit where each converter has its own controller to stabilize the output voltage and keeps the system operating on continuous conduction mode. Another control – based on predictive control system [17-18] – encompasses all controllers and updates the voltage reference of each controller.

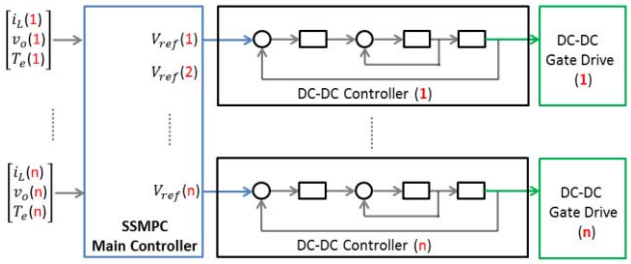

Fig. 6 – Control scheme proposed

A. Cascade control of converters - discharge mode

During the discharge mode operation, the control of the output voltage of each boost converter is implemented using a classic cascade control [20-22]. The current controller (inner loop) operates in higher speed than the voltage controller which has a non-minimal phase behavior.

B. Main controller based on prediction of SOC and Te

The prediction of the future states of SOC and T_e are made based on the SSMPC, using a dynamic reference. Fig. 7 shows a flowchart of the algorithm implemented to control the converter.

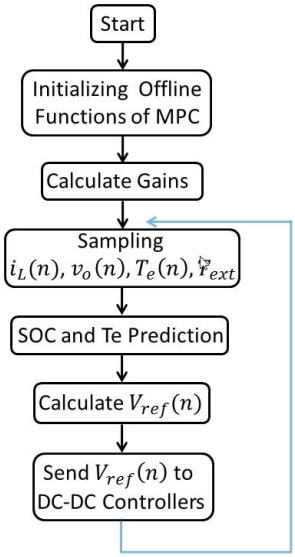

Fig. 7 – Predictive Algorithm

Each voltage reference value is calculated based on the future values of SOC(n) and T_e(n) predicted by the controller. There are limits of voltage reference variation that the controller must respect. These limits are based on maximum current of each battery which is the same current of the boost inductor. Based on it, the value of voltage reference is calculated by,

$$V_{ref\_SOC}(n) = \frac{\Delta_{Vref}(\max)}{\Delta_{SOC}(\max)}.\left(SOC_{fut}(k) - \overline{SOC_{fut}}(k)\right) + V_{Ref}^{p} \qquad (4)$$

The parcel of predicted temperature is also based on similar analysis. Batteries with higher internal temperature will suffer higher degradation than others. To prevent an abusive stress

on those cells, the controller manages the average temperature of the batteries, reducing the weight of their contribution to supply the load, which leads also in lower joule effect losses. The portion is calculated by,

$$V_{ref\_Te}(n) = \frac{\Delta_{Vref}(\max)}{\Delta_{Te}(\max)} \cdot \left(\overline{Te_{fut}}(k) - Te_{fut}(k)\right) + V_{Ref}^{p} \quad (5)$$

The controller also imposes thermal limits to avoid any of the cells operating out of the bounds. When the system operates inside the thermal limits, the controller will prioritize the SOC equalization of the system through the definition below, where $W_{SOC} > W_{Te}$.

$$V_{ref}(k,n) = \frac{W_{SOC} \cdot V_{ref\_SOC}(n) + W_{Te} \cdot V_{ref\_Te}(n)}{W_{SOC} + W_{Te}} \quad (6)$$

Otherwise, the thermal equalization will prioritize the value of reference voltage calculated by thermal prediction, resulting in $W_{Te} > W_{SOC}$. This mode will be sustained to the point that temperature reaches a lower level of T_e. When the difference in SOC is too large, the equalization speed will be dynamic changed to a slower level through the control of the $\Delta_{SOC}(\max)$ variable.

After that, the voltage reference of the converters is updated and the main controller refreshes its reference values for the next iteration. The references of predictive control will be reloaded as

$$Yref(k) = dSOC(k)$$
$$Yref(k) = dTe(k)$$

Where,

$$dSOC(k) = \frac{1}{\beta(T).Cap} \int_{0}^{Ta} \left(A_{fc}(n)I + B_{fc}(n)\right).I.dt \quad (7)$$

And

$$\beta(T) = F_T(n).Te_{fut}(n).Cap(n) \quad (8)$$

V. SIMULATION RESULTS

A simulation is preceded based on discharge mode of the system. A four-module system operating on discharge mode is simulated to introduce the topology and control method proposed in this paper. The characteristics of the system are presented below.

V_O = 24 V	[*Voltage reference*]
V_I = 12 V	[*Batteries voltage*]
V_L = 96 V	[*Load voltage – DC link*]
I_O = 0.5 A	[*Load current*]
η = 100%	[*Converter Efficiency*]
B_{cap} = 5 Ah	[*Battery Capacity*]
T_{ext} = 27 ºC	[*External temperature*]

A. Different SOC

The first basic test is to verify the behavior of system operating with SOC imbalance. Considering that all internal cells characteristics are equal and are the same at all time, the next table shows the initial condition of the SOC of each cell.

Battery (n)	1	2	3	4
Initial SOC	0.90	0.85	0.80	0.75

Tab. 1 – Initial SOCs condiction for simulation

The Fig. 8 shows the operation of all converters without the actions of the predictive control. All reference voltages are fixed at 24 V. Although the equalizer strategy is out of operation, the DC link is fixed at its level.

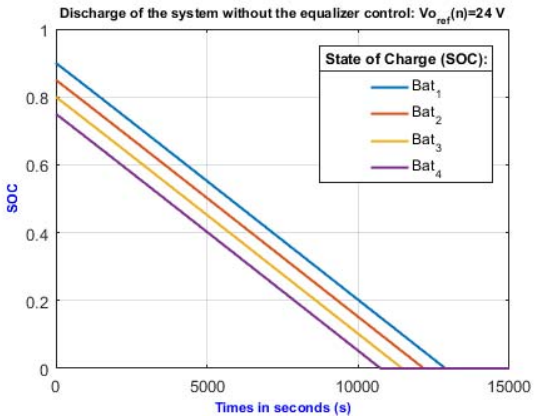

Fig. 8 – Discharge of the system without the equalizer control

Turning on the predictive equalizer control, a further step was taken with a new simulation, with the same conditions as previously. Fig. 9 shows the dynamic adjustment of the reference voltage (V_{ref}). The load connected is constant during all period, and the weight of SOC equalization is fixed at 4.0, which means that SOC prediction is four times more relevant than the internal temperature prediction to determine the new values of V_{ref}. Other settings are displayed at the next table.

$\Delta_{SOC}(\max) = 0.02$	$\Delta_{Vref}(\max) = 9V$	$\Delta_{Te}(\max) = 1$°C

Tab. 2 – Settings parameters

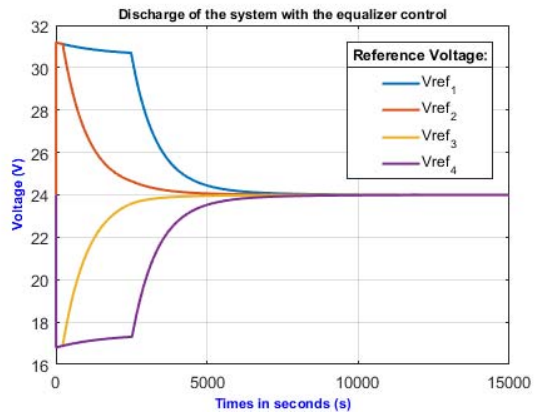

Fig. 9 – Reference voltages during equalizer discharge mode

The State of Charge of the batteries is showed in Fig. 10, where the equalization is complete at 1h:18min, and the

system operated for 3h:16min, which corresponds 17.45 minutes more than the system without equalization control. It represents 50.25 kJ more energy transferred to the load, which it is approximately 9.75% more than a system without the equalizer.

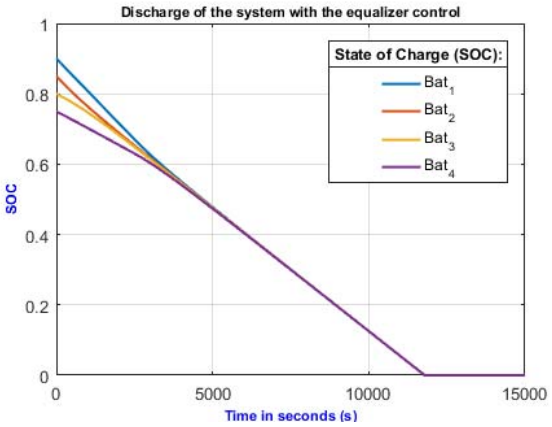

Fig. 10 – Discharge of SOC with equalizer control

B. *Speed of equalization*

The process of equalization can be accelerated through the change of the parameters W_{soc} and T_{soc}, but specially with the variations of the maximum limits of the Δ_{soc} and Δ_{Te}. The Tab. 3 presents an example of variation of the equalization time through the variation of W_{soc} ($T_{soc} = 1$) considering the simulation of the system presented in A. Also, in the Tab. 4, shows the variation of the equalization time through the variation of Δ_{soc}, where Δ_{Te} is fixed at 1°C.

$\Delta_{Te} = 1\,°C$	
$\Delta_{soc} = 0.02$	
W_{SOC}	$T_{eq}(s)$
1	*8871*
2	*6155*
3	*5210*
4	*4735*

Tab. 3- Example of W_{soc} variation

$W_{Te} = 1$	
$W_{SOC} = 4$	
Δ_{soc}	$T_{eq}(s)$
0.01	*3692*
0.02	*4735*
0.04	*7353*
0.08	*11787*

Tab. 4 - Example of Δ_{soc} variation

In a very imbalance condition, the speed of equalization is dynamically changed, as it can be seen in the green curve of the simulation presented in Fig 11. The initial unbalanced SOCs are show in Tab. 5.

Battery (n)	1	2	3	4
Initial SOC	0.90	0.70	0.70	0.70

Tab. 5 – Initial SOCs condiction for simulation

The speed of the process is reduced during the process to avoid an unstable behavior of the system.

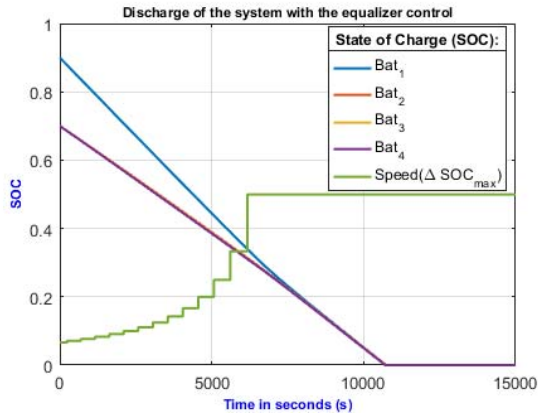

Fig. 11 – Speed variation during the discharge and equalization process

Otherwise, the controller projected would not be able to stabilize the voltage output of the system without this dynamic speed control. The voltage output of the system, in this case is equal to $V_{out} = 96\,V$, as it is showed stabilized through all the process at Fig 12.

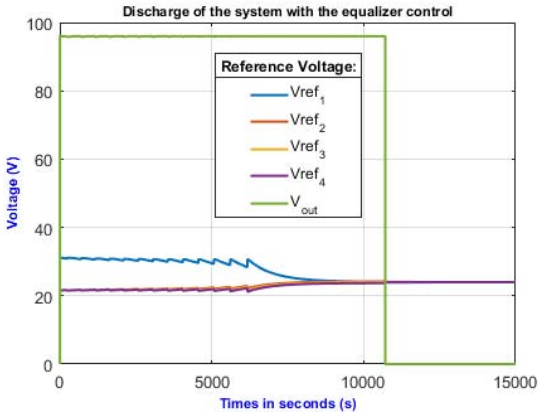

Fig. 12 – Stabilization of the output voltage through the variation of the speed equalizer

C. *Different internal characteristics of cells*

The prediction behavior of the controller allows it to avoid future unbalances even when the characteristics of cells are not the same, it is true as long as the parameters are monitored and the curve models of each cell reconfigured. Considering a constant factor that affects the capacity curve of batteries, a different value is established for each cell during the next simulation.

$$\eta(n) = K_T(n).(A_{fc}I + B_{fc})$$

Battery (n)	1	2	3	4
Temp Factor (K_T)	0.0040	0.0036	0.0034	0.0037

Tab. 6 – Initial SOCs condiction for simulation

The cell 1 is the unhealthy cell, and the system naturally will lose its equilibrium along the discharge time due to these internal differences, which is a more realistic operation of the batteries.

Battery (n)	1	2	3	4
Initial SOC	0.90	0.90	0.90	0.90

Tab. 7 – Initial SOCs condiction for simulation

Fig. 13 shows the simulation without the operation of the equalizer. As time went on, the SOC of the cells become unbalanced due their internal differences. Although the simulation has parameters that acellerate this unbalancing process, this kind of behavior is going to happen in a real system for a number of reason, like the difference between SOH cells and condictions of use.

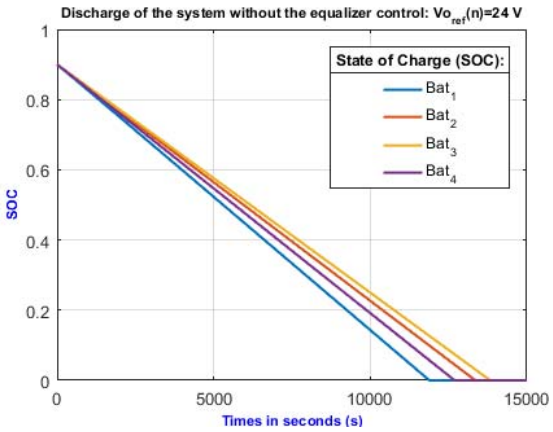

Fig. 13 – Discharge of the system without the equalizer control

Realizing a new simulation considering the actions of the equalizer controller, the system does not allow the cells to becomes unbalanced over the time, as the simulation showed in Fig. 14.

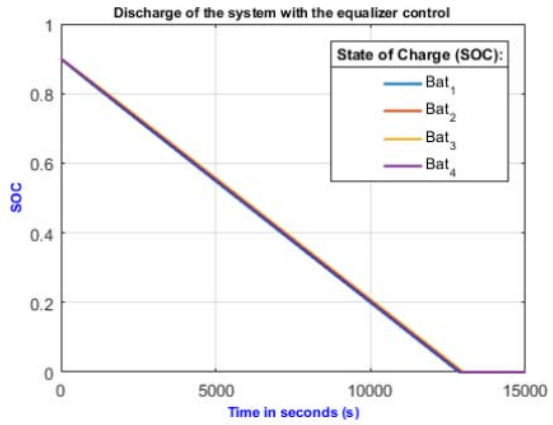

Fig. 14 – Discharge of the system with the equalizer control

The parameters $K_T(n)$ can be used to monitor the degradation of each cell. [19] Implantation of the parameters monitoring (Rin, Co and Ro) of battery can dynamically operate with the controller to avoid the natural imbalance of the system even when the cells degrade, but it's a case for a future study.

VI. CONCLUSION

The modularized scheme is an alternative topology to the series cell systems that need a step-up converter to reach the level voltage of the DC link, reducing the number of series cells needed. The modularization of the system allows it to work as an individual or modularized active equalizer, which the use of just one central converter could not provide. Also the equalizer doesn't need to transfer energy from a bank to another as the most active equalizer systems does, and it results in lower energy losses. The use of this system can result in extending the cells life through the control of the energy levels that cause their degradation during charges and discharges. Finally, as a future work, the proposed system will be implemented to evaluate the models and the general performance.

VII. REFERENCES

[1] Ling, R., et al. (2015). A review of equalization topologies for lithium-ion battery packs. Control Conference (CCC), 2015 34th Chines

[2] Hung, S. T., Hopkins, D. C., Mosling, C. R. (1993). "Extension of battery life via charge equalization control." Industrial Electronics, IEEE Transactions on 40(1): 96-104.

[3] Hoke, A., et al. (2013). Maximizing lithium ion vehicle battery life through optimized partial charging. Innovative Smart Grid Technologies (ISGT), 2013 IEEE PES.

[4] Pascual, C. and P. T. Krein (1997). Switched capacitor system for automatic series battery equalization. Applied Power Electronics Conference and Exposition, 1997. APEC '97 Conference Proceedings 1997., Twelfth Annual.

[5] Tae-Hoon, K., et al. (2012). Low cost multiple zero voltage/zero current switching battery equalization circuit with single soft-switching resonant cell. 2012 IEEE Vehicle Power and Propulsion Conference.

[6] Karnjanapiboon, C., et al. (2003). The low stress voltage balance charging circuit for series connected batteries based on buck-boost topology. Circuits and Systems, 2003. ISCAS '03.

[7] Ming, T. and T. Stuart (2000). "Selective buck-boost equalizer for series battery packs." Aerospace and Electronic Systems, IEEE Transactions on 36(1): 201-211.

[8] Feng, J., et al. (2014). Modularized global equalization of battery cells for electric vehicles. Robotics and Automation (ICRA), 2014 IEEE International Conference on.

[9] Hong-sun, P., et al. (2009). "Design of a Charge Equalizer Based on Battery Modularization." Vehicular Technology, IEEE Transactions on 58(7): 3216-3223.

[10] Ju, F., et al. (2016). "Performance Evaluation of Modularized Global Equalization System for Lithium-Ion Battery Packs." IEEE Transactions on Automation Science and Engineering 13(2): 986-996.

[11] Lee, Y.-S. and C. Ming-Wang (2005). "Intelligent control battery equalization for series connected lithium-ion battery strings." Industrial Electronics, IEEE Transactions on 52(5): 1297-1307.

[12] Anno, T. and H. Koizumi (2013). Bidirectional chopper using cell voltage equalizing with flyback transformer. Industrial Electronics Society, IECON 2013 - 39th Annual Conference of the IEEE.

[13] Shichuan, D., et al. (2010). A hybrid-source switched-capacitor multilevel converter for electric vehicles. Electrical Machines and Systems (ICEMS), 2010 International Conference on.

[14] Li, Y. and Y. Han (2015). Control of input-series and output-independent power converter building block system based on buck converter topology. 2015 IEEE

[15] Gaffar, M. A., et al. (2016). Simulink based performance analysis of lead acid batteries with the variation of load current and temperature. 2016 4th International Conference on the Development in the in Renewable Energy Technology (ICDRET).

[16] Guo, L., et al. (2015). The SOC estimation of battery based on the method of improved Ampere-hour and Kalman filter. 2015 IEEE 10th Conference on Industrial Electronics and Applications (ICIEA).

[17] J.M. Maciejowski, Predictive control with constraints, Prentince Hall, 2000.

[18] J. Rodriguez and P. Cortes, Predictive Control of Power Converters and Electrical Drives. Wiley, 2012.

[19] Nakajo, K., et al. (2016). On-line measurement system for internal resistance in lead acid battery. 2016 55th Annual Conference of the Society of Instrument and Control Engineers of Japan (SICE).